Control of Redundantly Actuated PKMs for Closed-Shape Trajectories Tracking with Real-Time Experiments

Moussab Bennehar, Ahmed Chemori, François Pierrot, Sébastien Krut

M. Bennehar, A. Chemori, F. Pierrot and S. Krut

Control of Redundantly Actuated PKMs for Closed-Shape Trajectories Tracking with Real-Time Experiments

Abstract: This paper deals with closed-shape geometric reference trajectories generation and dynamic control of redundantly actuated parallel kinematic manipulators. Geometric trajectories if generated by means of trigonometric functions may show inherent discontinuities regarding velocities and/or accelerations which may cause problems for the drives. In order to overcome this issue and to generate C^2 continuous refernce trajectories, we propose a novel technique consisting of modifying the motion profile while preserving the overall geometric shape of the trajectory in the operational space. Regarding the control strategy and to deal with the actuation redundancy, an extended version of the PD controller with computed feedforward is proposed. The computed control inputs, before being applied to the actuators, are first projected using a regularization matrix based on the manipulator's kinematics in order to remove the antagonistic internal forces. The overall proposed strategy including the trajectory generator as well as the controller are experimentally validated on the Dual-V robot, a three-degree-of-freedom redundantly actuated parallel kinematic manipulator developed in our laboratory.

Keywords: Parallel manipulators, trajectory generation, dynamics, control.

1 Introduction

Parallel Kinematic Manipulators (PKMs) are mostly known for their superior dynamic performance compared to their serial counterparts [1]. Indeed, in contrast with serial manipulators in which the actuators are located on the moving links, the actuators in the case of PKMs are located on the fixed base resulting in a much lighter moving parts. Consequently, PKMs can achieve extremely high velocities and accelerations [2]. Furthermore, the closed kinematic chains structure of PKMs yields more stiffness, better accuracy and a higher load/weight ratio [1]. Nevertheless, PKMs exhibit some drawbacks that may moderate their expansion in industrial applications. The abundance of singularities and the relatively small workspace are the most noteworthy limitations. While the latter is a matter of mechanical design, the former can be solved through actuation redundancy. For this reason, Redundantly Actuated

M. Bennehar, A. Chemori, F. Pierrot and S. Krut: LIRMM, UMR 5506,CNRS Université de Montpellier II, 161 rue Ada, 34392 Montpellier cedex 5, France, emails: ahmed.chemori@lirmm.fr, mbennehar@gmail.com

PKMs (RA-PKMs) have increasingly attracted the interest of researchers over the last two decades. Actuation redundancy significantly improves the performance of PKMs by homogenizing the dynamic properties throughout the workspace, allowing the manipulator to achieve very high accelerations in all configurations. However, despite the aforementioned qualities, PKMs potential is not yet completely explored and is still an open research area. From one hand, mechanical design, identification and optimization can be further investigated to achieve more efficient prototypes for industrial community. From the other hand, the constraints involved by the closed kinematic chains and the high nonlinear dynamics give rise to more challenging problems in terms of trajectory generation and control that earn to be studied.

Thanks to their extremely high dynamic capabilities, PKMs are typically used for high-speed industrial applications such as pick-and-place in food industry [3] and the assembly of electronic components [4]. Consequently, the most used solutions in terms of trajectory generation are based on traditional Point-to-Point (PtP) trajectories. In [5], an online smooth jerk-bounded trajectory generator using fifth order polynomials was proposed. The jerk boundedness yields an improved path tracking and a reduced wear on the robot. The problem of time optimality of PtP trajectories was addressed in [6]. An algorithm to derive the optimal trajectory was proposed and experimentally implemented on a 2-degree-of-freedom PKM. In [7], a variety of pick-and-place trajectory planners were evaluated with the aim of reducing vibrations of an elastic five-bar mechanism. Though the trend in this research area is towards PtP and pick-and-place trajectories, the inherent superior qualities of PKMs award them to be used in more complex modern industrial tasks such as laser cutting [8], machining [9] or even medical applications [10]. In this case, Geometric Closed Shape (GCS) trajectories draw more attention than traditional PtP ones [11]. This class of trajectories however, has not been sufficiently investigated in the literature. Indeed, in order to be better tracked by the robot's end effector (a traveling plate in the case of PKMs), the generated trajectories have to satisfy continuity constraint and respect the dynamic capabilities of the manipulator.

In order to track the reference trajectories with the best tracking performance, an efficient control scheme should take into account the nonlinear dynamics of the robot manipulator. Even if PKMs have different kinematics than serial manipulators, they actually share many dynamic similarities. Consequently, most of the developed control schemes for serial manipulators have been straightforwardly implemented on fully actuated PKMs [12–14]. However, in the case of RA-PKMs, a particular property characterizing this class of manipulators needs a special attention. Indeed, the non-uniqueness of the inverse dynamics solution yields antagonistic control forces that have no effect on the motion of the mechanical structure [15]. These control forces produce undesired internal pre-stress in the kinematic chains which may damage the manipulator, cause a loss of energy and generate mechanical vibrations. Consequently, a good control scheme should take into consideration such a phenomenon.

In this work, we address the two aforementioned issues namely, the continuous GCS trajectories generation and the internal forces free control of RA-PKMs. We propose herein a trajectory generator that takes into consideration continuity constraints in velocities and accelerations, both in task and joint spaces. Regarding the control solution, a joint space PD controller with computed feedforward [16] is proposed. This control scheme has the advantage of being low computationally efficient while compensating for some of the nonlinearities in the dynamics. In order to deal with the internal forces issue, the proposed controller is enhanced by a projection of the generated control torques with the seek of regularization. The proposed control scheme is then validated through real-time experiments on a 3-dof RA-PKM named Dual-V.

The rest of the paper is organized as follows. In section 2, the dynamic model of the Dual-V robot is presented. Section 3 is devoted to the proposed trajectory generator. The proposed control solution is detailed in Section 4. Experimental results are presented in Section 5. Finally, conclusions and perspectives are addressed in Section 6.

2 Description and Dynamic Modeling of the Dual-V Manipulator

Dual-V robot is a 3-dof planar RA-PKM belonging to the 4-RRR family. The arrangement of its four closed kinematic chains allows three independent movements for its traveling plate: two translations throughout the plane and one rotation about the z-axis. Hence, the Cartesian coordinates of the traveling plate can be described by the vector $X = [x, y, \theta]^T \in \mathbb{R}^3$. Regarding the dynamic modeling of the robot, the approach developed in [2] has been extended to take into account the rotational inertia of the forearms.

The input torque vector required to move the robot's mechanical structure $\Gamma \in \mathbb{R}^4$ is decomposed into three main sub-torques namely: γ_1, γ_2, $\gamma_3 \in \mathbb{R}^4$. Each sub-torque is responsible for moving specific parts of the mechanical structure of the robot as follows: the torque γ_1 is the required torque to move the traveling plate and a part of the couplers, it can be calculated using the equations of power of the actuators, it is given by:

$$\gamma_1 = J_m^{T*} M_I \ddot{X} \tag{1}$$

where $M_I \in \mathbb{R}^{3\times3}$ is the mass matrix of the traveling plate and a part of the cranks being expressed in Cartesian space, $J_m^{T*}(q) \in \mathbb{R}^{4\times3}$ is the pseudo-inverse of the transpose of the *inverse Jacobian matrix* J_m and $\ddot{X} \in \mathbb{R}^3$ is the Cartesian acceleration vector of the traveling plate. The sub-torque γ_2 is the required torque to move the cranks, the

counter-masses and the remaining part of the couplers, it can be expressed as:

$$\gamma_2 = M_{II}\ddot{q} = M_{II}(\dot{J}_m\dot{X} + J_m\ddot{X}) \tag{2}$$

where $M_{II} \in \mathbb{R}^{4\times4}$ is the mass matrix including the dynamic parameters of the involved moving parts of the mechanical structure being expressed in joint space, $\dot{X} \in \mathbb{R}^4$ is the traveling plate velocity vector and $\dot{J}_m(q, \dot{q})$ is the time derivative of the inverse Jacobian matrix.

Up to now, only the inertia of the equivalent two-mass model [17] of each coupler is considered. In fact, the mass of each coupler is split up into two point-wise masses located at both ends of the considered link. Then, the rotational inertia of the two-mass model is considered instead of the real inertia of the couplers. Though this is a righteous assumption when light materials are used, it fails when the links are made with relatively heavy materials. This is the case of Dual-V parallel manipulator robot and hence, an additional term should be added. The sub-torque γ_3 is the additional torque component which accounts for the difference between real inertia and the one of the equivalent mass model of the couplers. Due to limitation on the number of pages, the details of this additional term are omitted and the interested reader is referred to [17] for a full description of the Dual-V robot dynamic modeling. It is worth noting though that $\gamma_3 = f(X, \dot{X}, \ddot{X})$ is a highly nonlinear function with respect to its arguments.

Finally, the full dynamic model of the Dual-V is obtained by summing the three sub-torques as follows:

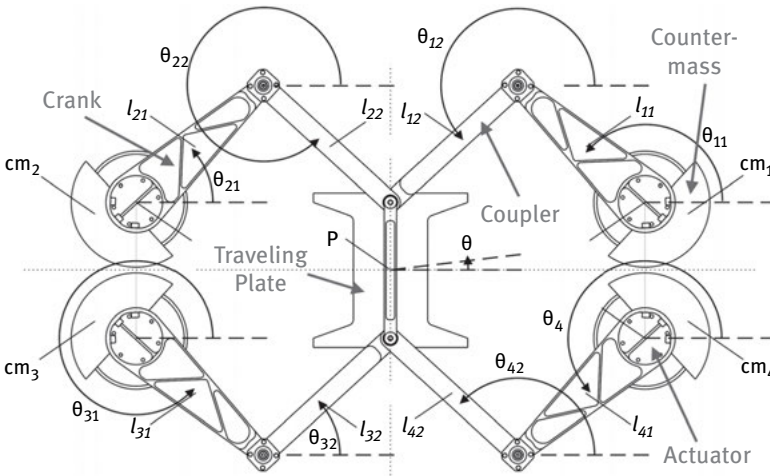$$\Gamma = J_m^{T*} M_I \ddot{X} + M_{II}(\dot{J}_m\dot{X} + J_m\ddot{X}) + \gamma_3 \tag{3}$$

Fig. 1. CAD view of Dual-V parallel manipulator and its parameters definition.

Tab. 1. Dual-V geometric and dynamic parameters.

	Length [m]	Mass [Kg]	Inertia [Kgm^2]
Crank	0.2800	1.169	0.012967
Coupler	0.2800	0.606	0.006417
Traveling plate	0.22	0.899	0.008168

The CAD model of the Dual-V with its parameters' definition is illustrated in Fig. 1; its geometric and dynamic parameters are summarized in Tab. 1. Further details regarding the Dual-V parallel manipulator can be found in [18] and [19].

3 C^2 Reference Trajectories Generation

Geometric Closed Shape trajectories are more complex than traditional PtP ones [5, 6] (e.g pick-and-place trajectories) and, in most cases, are generated by means of trigonometric functions parametrized by the time variable $t \in \mathbb{R}^+$. Generating trajectories with C^2 continuity constraints (i.e. on velocities and accelerations) may not be possible using standard analytical equations. Continuity of trajectories is a crucial constraint for the robot drives and actuators and is required in most robotic applications. Indeed, discontinuities in the trajectories may generate discontinuous control inputs and consequently, lead to undesired behavior of the mechanical structure such as mechanical vibrations, poor tracking performance and instabilities.

In this paper we are interested in the class of trajectories described by a sum of weighted sine and cosine functions. This class of trajectories has been chosen because it covers a large amount of geometric shapes from basic to the most complex ones (e.g. circles, ellipses, deltoids, ...).

The general analytical form of the trajectories in question is then expressed by:

$$x(t) = \sum_{i=1}^{n} a_i \cos^{\alpha_i}\left(2\pi \frac{n_{1i}}{T} t\right) + b_i \sin^{\beta_i}\left(2\pi \frac{n_{2i}}{T} t\right) \tag{4}$$

where $T \in \mathbb{R}^+$ is the trajectory duration and $a_i,\ \alpha_i,\ b_i,\ \beta_i,\ n_{ji} \in \mathbb{R}; i = 1, \dots, n; j = 1, 2$ are scalars defining the overall shape of the trajectory.

In the sequel, we will first give an illustrative example of direct application of (4). Then, its major drawback is highlighted and a solution to overcome this issue is proposed.

3.1 Trajectories using Standard Geometric Functions

Let $x_d(t)$ be a reference Cartesian position defined by (4) to be tracked by the traveling plate of the robot. It is assumed throughout this brief that the reference trajectories are inside the workspace of the robot and hence are away from singularities. The reference velocity $v_d(t)$ and acceleration $a_d(t)$ for this motion are obtained by differentiating $x_d(t)$ with respect to time, giving thus:

$$v_d(t) = -\frac{2\pi}{T} \sum_{i=1}^{n} a_i \alpha_i n_{1i} \sin^{\alpha_i-1}\left(2\pi\frac{n_{1i}}{T}t\right) - b_i \beta_i n_{2i} \cos^{\beta_i-1}\left(2\pi\frac{n_{2i}}{T}t\right) \tag{5}$$

$$a_d(t) = -\left(\frac{2\pi}{T}\right)^2 \sum_{i=1}^{n} a_i \alpha_i (\alpha_i-1) n_{1i}^2 \cos^{\alpha_i-2}\left(2\pi\frac{n_{1i}}{T}t\right)$$

$$+ b_i \beta_i (\beta_i-1) n_{2i}^2 \sin^{\beta_i-2}\left(2\pi\frac{n_{2i}}{T}t\right) \tag{6}$$

Without loss of generality, assume that the manipulator starts and finishes its movement with zero velocity and acceleration (i.e. $v(0) = v(T) = 0$ and $a(0) = a(T) = 0$). However, using the original analytical functions (5) and (6) may lead to non-zero initial velocity and/or acceleration and thus, discontinuities in the generated motion. Indeed, if we replace $t = 0$ or $t = T$ in (5) and (6) we will obtain values dependent on initial and final conditions and thus, do not necessarily equal to zero. For instance, the obtained initial conditions for (5) and (6) are given by:

$$v_d(0) = -\frac{2\pi}{T} \sum_{i=1}^{n} b_i \beta_i n_{2i} = f_1(b_i, \beta_i, n_{2i}) \tag{7}$$

and

$$a_d(0) = -\left(\frac{2\pi}{T}\right)^2 \sum_{i=1}^{n} a_i \alpha_i (\alpha_i-1) n_{1i}^2 = f_2(a_i, \alpha_i, n_{1i}) \tag{8}$$

therefore, the resulting trajectories can be discontinuous in velocity and/or acceleration leading to discontinuous control torques and therefore big tracking errors and even problem of vibrations.

To further illustrate this inconvenience let's consider a simple circular trajectory with radius $r \in \mathbb{R}^+$ and a center whose coordinates are $(x_c, y_c) = (0, 0)$. The resulting trajectory needs to be C^2 continuous (in velocities and accelerations) both in operational and joint spaces in order to be appropriately tracked by the proposed controller. The analytical equations of positions, velocities and accelerations are given by:

$$\begin{cases} x_d(t) &= r \cos\left(\frac{2\pi}{T}(t-t_0)\right) \\ y_d(t) &= r \sin\left(\frac{2\pi}{T}(t-t_0)\right) \end{cases} \tag{9}$$

$$\begin{cases} \dot{x}_d(t) &= -r\frac{2\pi}{T} \sin\left(\frac{2\pi}{T}(t-t_0)\right) \\ \dot{y}_d(t) &= r\frac{2\pi}{T} \cos\left(\frac{2\pi}{T}(t-t_0)\right) \end{cases} \tag{10}$$

$$\begin{cases} \ddot{x}_d(t) &= -r(\frac{2\pi}{T})^2 \cos\left(\frac{2\pi}{T}(t - t_0)\right) \\ \ddot{y}_d(t) &= -r(\frac{2\pi}{T})^2 \sin\left(\frac{2\pi}{T}(t - t_0)\right) \end{cases} \tag{11}$$

These trajectories satisfy equations (4), (5) and (6) being only shifted in time by t_0. Figure 2 illustrates the plots of the obtained trajectories using (9), (10) and (11) for the parameters $t_0 = 0.5s$, $T = 1s$. It can be clearly noticed the presence of discontinuities on both velocity and acceleration profiles that have to be removed. In what follows, we propose a novel method to overcome this drawback and generate C^2 continuous reference trajectories.
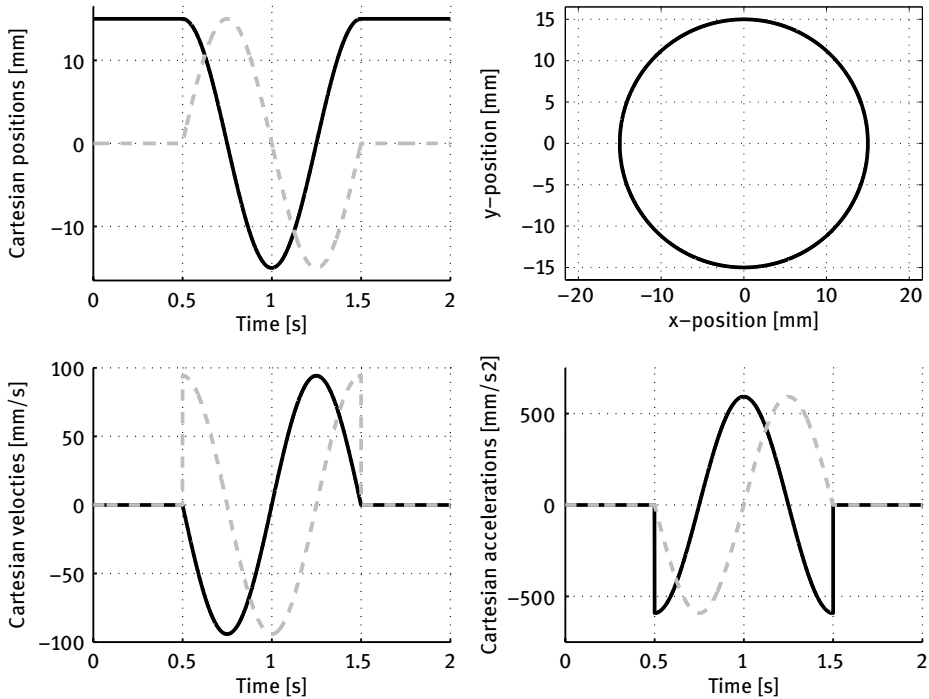

Fig. 2. View of the generated Cartesian trajectories using standard geometric functions. x_d (solid) and y_d (dashed).

3.2 Proposed C^2 Continuous Reference Trajectories

In order to overcome the discontinuity problem in the velocity and acceleration trajectories, we propose to revisit the analytical form of the desired operational trajectories. Consider again the previous illustrative example of the circular trajectory.

If we check the previous equations of the trajectory, it can be seen that they can be rewritten as follows:

$$\begin{cases} x_d(t) &= & r\cos(\lambda(t)) \\ y_d(t) &= & r\sin(\lambda(t)) \end{cases} \tag{12}$$

with $\lambda(t) = \frac{2\pi}{T}(t - t_0)$ which is a simple affine function of time t and when implemented, does not satisfy any continuity constraints on the velocities and accelerations. The corresponding velocities and accelerations can be obtained by differentiating (12) with respect to time, which gives:

$$\begin{cases} \dot{x}_d(t) &= & -r\,\dot{\lambda}(t)\,\sin(\lambda(t)) \\ \dot{y}_d(t) &= & r\,\dot{\lambda}(t)\,\cos(\lambda(t)) \end{cases} \tag{13}$$

$$\begin{cases} \ddot{x}_d(t) &= & -r\left[\ddot{\lambda}(t)\sin(\lambda(t)) + \dot{\lambda}^2(t)\cos(\lambda(t))\right] \\ \ddot{y}_d(t) &= & r\left[\ddot{\lambda}(t)\cos(\lambda(t)) - \dot{\lambda}^2(t)\sin(\lambda(t))\right] \end{cases} \tag{14}$$

From (13) and (14) one can notice that if $\lambda(t)$ is chosen such that it satisfies the following boundary constraints:

$$\begin{cases} \lambda(t_0) = 0, & \dot{\lambda}(t_0) = 0, & \ddot{\lambda}(t_0) = 0 \\ \lambda(t_0 + T) = 2\pi, & \dot{\lambda}(t_0 + T) = 0, & \ddot{\lambda}(t_0 + T) = 0 \end{cases} \tag{15}$$

one can ensure the continuity on the velocity and acceleration trajectories. One possible solution would then be to choose $\lambda(t)$ with a trapezoidal velocity profile. Indeed, this choice allows to specify boundary conditions and hence, the constraints (15) can be satisfied. A comparison between trapezoidal and linear velocity profile for $\lambda(t)$ is depicted in Fig. 3. The analytical equations of $\lambda(t)$ are now expressed as:

$$\begin{cases} \lambda(t) &= & \frac{\lambda_f - \lambda_0}{2\tau^3(T - \tau)}[-t^4 + 2\tau t^3] + \lambda_0, & t_0 \le t < \tau \\ \lambda(t) &= & \frac{\lambda_f - \lambda_0}{(T - \tau)}[t - \frac{\tau}{2}] + \lambda_0, & \tau \le t < T - \tau \\ \lambda(t) &= & \frac{\lambda_f - \lambda_0}{2\tau^3(T - \tau)}[(t - T)^4 + 2\tau(t - T)^3] + \lambda_f, & \text{otherwise} \end{cases} \tag{16}$$

where τ is the duration of initial acceleration and final deceleration phases that has to be chosen according to the robot dynamic capabilities (choosing small values for τ may lead to unachievable high accelerations). λ_0 and λ_f are the initial and final values respectively for $\lambda(t)$ which depend on the type of the geometric trajectory. For instance, in the case of the previous circular trajectory example, $\lambda_0 = 0$ and $\lambda_f = 2\pi$.

The obtained trajectories using the proposed technique as depicted in Fig. 4 are now continuous in velocity and acceleration and result in the same circular trajectory in operational space as the original one. Therefore, they are more safe in the control scheme for the actuators of the robot manipulator.
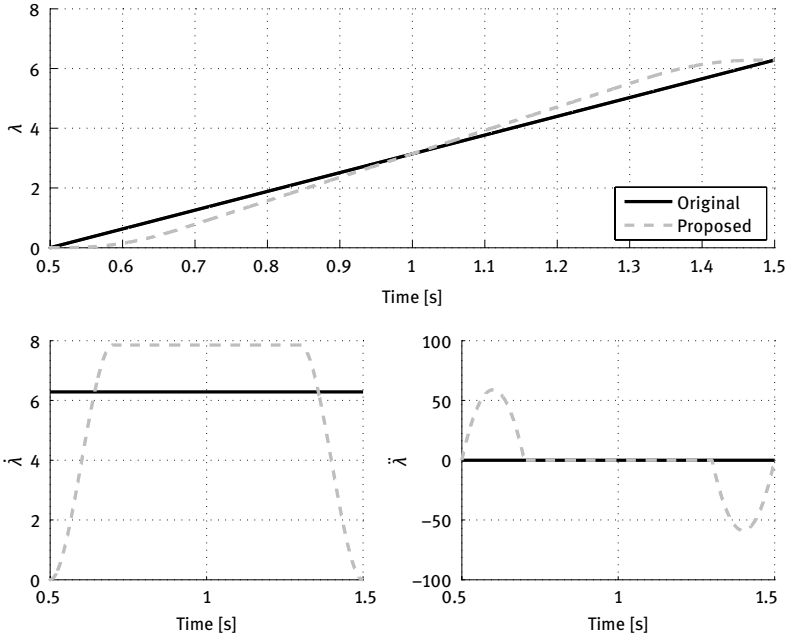
Fig. 3. Evolution of $\lambda(t)$, $\dot{\lambda}(t)$ and $\ddot{\lambda}(t)$ versus time.
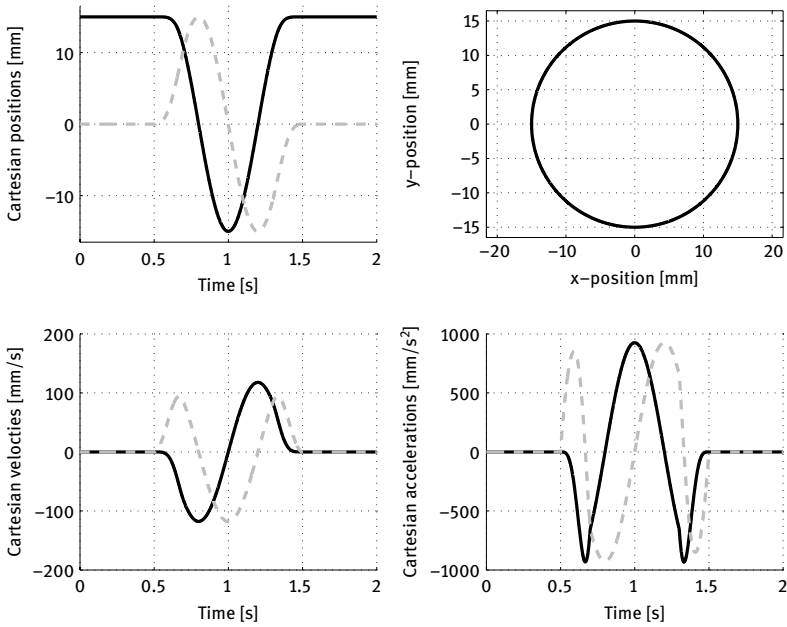

Fig. 4. Obtained C^2 continuous operational trajectories. x_d (solid) and y_d (dashed).

4 Proposed Control Solution

It is conventional that PKMs share many similarities with their serial counterparts regarding dynamic properties [14]. Consequently, the vast wide control literature developed for serial manipulators can be successfully applied to PKMs. However, in the particular case of RA-PKMs, the use of decentralized single axis controllers leads to antagonistic control efforts. Indeed, these efforts do not produce any motion of the manipulator. Thus, using conventional single axis strategies in the control loop will certainly involve internal forces (incompatible with the robot's kinematics) [15] creating internal pre-stress in the mechanism. The antagonistic forces can cause a multitude of undesirable phenomena such as loss of energy, instability and even mechanical vibrations. Consequently, the control architecture when designed has to take this issue in consideration. In this work we propose to enhance the well known PD controller with computed forward by projecting the computed inputs in order to reduce the effect of antagonistic forces. Figure 5 shows an overview of the different components of the proposed control scheme.
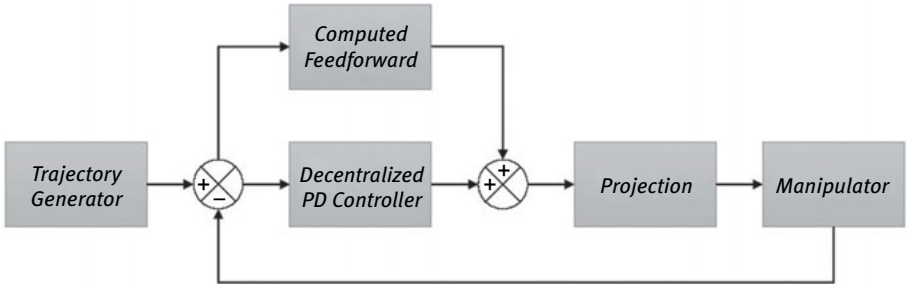

Fig. 5. Overview of the proposed control architecture.

4.1 Decentralized Joint Space PD Controller

Consider a RA-PKM with m degrees of freedom and n actuators and let the joints position vector be denoted by $q \in \mathbb{R}^n$. The PD control in joint space is a decentralized uncoordinated control strategy relying on the measured errors between the desired and the actual positions. Let $e(t) = q_d(t) - q(t)$ be the vector of joints errors, where $q_d(t)$ denotes the desired joint trajectory. Then, the PD control action is expressed by:

$$\Gamma_{PD} = K_p e(t) + K_d \dot{e}(t) \tag{17}$$

where K_p and K_d are positive feedback gains usually chosen as diagonal matrices. If all the actuators are identical, which is usually the case for PKMs, then the same feedback

gains could be used for all axes, namely; $K_p = k_p I_{n \times n}$ and $K_d = k_d I_{n \times n}$, where $I_{n \times n}$ denotes the identity matrix and $k_p, \ k_d \in \mathbb{R}$ are positive scalars denoting the feedback gains that should be carefully tuned to achieve satisfactory tracking performance. A good accuracy is usually required in parallel robots; however, a PD controller is not able to assure that. Consequently, a computed feedforward is proposed to improve the tracking performance of the PD controller.

4.2 Tracking Accuracy Improvement through a Computed Feedforward

If the inverse dynamic model of the robot is known and its parameters are accurate enough, it would be interesting to exploit this knowledge in the control scheme to further improve the tracking performance. Indeed, the tracking errors can be significantly reduced by compensating the inherent nonlinear dynamics of the robot. One possible way would be the addition of a feedforward term. This strategy enables partial compensation of the nonlinear dynamics, i.e. only desired values of positions, velocities and accelerations are fed to the model-based term of controller. For the case of the Dual-V robot, the inverse dynamics are given by (3), hence, the feedforward control term can be expressed as:

$$\Gamma_{ff} = J_m^{T*}(q_d) M_I \ddot{X}_d + M_{II}(\dot{J}_m(q_d, \dot{q}_d) \dot{X}_d + J_m(q_d) \ddot{X}_d) + \gamma_{3_d} \tag{18}$$

where the subscript d refers to the desired quantities and $\gamma_{3_d} = f(X_d, \dot{X}_d, \ddot{X}_d)$.

4.3 Projection Method to Reduce Internal Forces

For RA-PKMs, the control inputs resulting from single axis controllers (i.e. PD portion) may contain antagonistic forces. These control inputs do not create any motion as they are in the null-space of J_m^T. However, they create uncontrolled internal pre-stress that may damage the manipulator. This issue has to be considered in the control architecture. One way to reduce the internal forces is by projecting the computed inputs onto the range of J_m^T by the following projector: [15]

$$R_{J_m^T} = I - N_{J_m^T} \tag{19}$$

where $N_{J_m^T} = I - J_m^{T*} J_m^T$ is the projector to the null-space of J_m^T. Hence, the internal antagonistic forces are eliminated by projecting the control torques onto the range space of J_m^T. This can be achieved using the projection matrix $R_{J_m^T}$ as:

$$\Gamma^* = R_{J_m^T}(\Gamma_{PD} + \Gamma_{ff}) \tag{20}$$

The overall block diagram of the proposed control scheme is illustrated in Fig. 6.
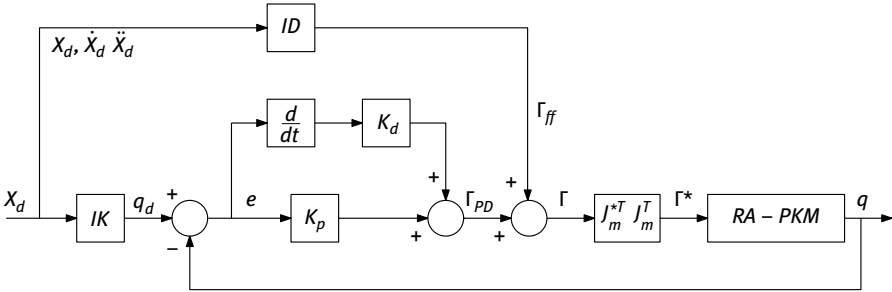

Fig. 6. Block diagram of the proposed control scheme; IK denotes the inverse kinematic model and ID the inverse dynamic model.

5 Real-Time Experimental Validation

5.1 Experimental Setup

All the links of the Dual-V are made of Aluminum. The cranks are mounted on four direct drive actuators manufactured by ETEL Motion Technology. The actuators are fixed on an Aluminum base and they can supply torques up to 127 N.m. Matlab software and Real-Time Workshop (both from Mathworks Inc.) have been used to implement and execute in real-time the proposed control scheme. The generated C code is then uploaded to the target PC (an industrial computer cadenced at 10 kHz and running xPC Target in real-time). The experimental setup is displayed in Fig. 7.

5.2 Obtained Experimental Results

The proposed trajectory generator and controller presented in the previous section were implemented on the Dual-V experimental testbed. For comparison purpose, we also implement the classical trajectories generator. In order to further investigate the benefits of the proposed approach, four different geometric shapes are included in the reference trajectories generator as illustrated in Fig. 8. The resulting reference trajectories include a circle, an ellipse, a tear-like and a deltoid geometric shapes. The traveling plate of the manipulator has to track each geometric trajectory in $T = 0.5\ s$. Between the end point of one closed-shape and the starting point of the next one,

Fig. 7. View of the experimental setup of Dual-V PKM; (1) the mechanical structure of the robot, (2) the host PC, (3) the target PC, (4) emergency stop, (5) host monitor, (6) xPC target monitor.
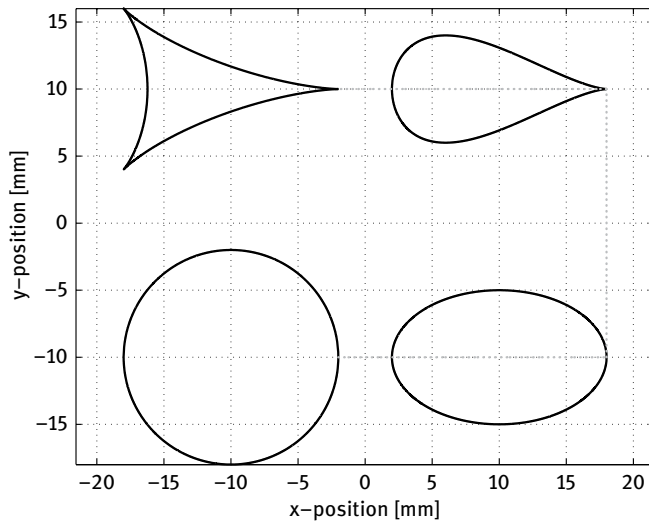

Fig. 8. Reference Cartesian trajectory used in experiments.

the end-effector has to perform a pick-and-place PtP trajectory defined by a 5th order polynomial function.

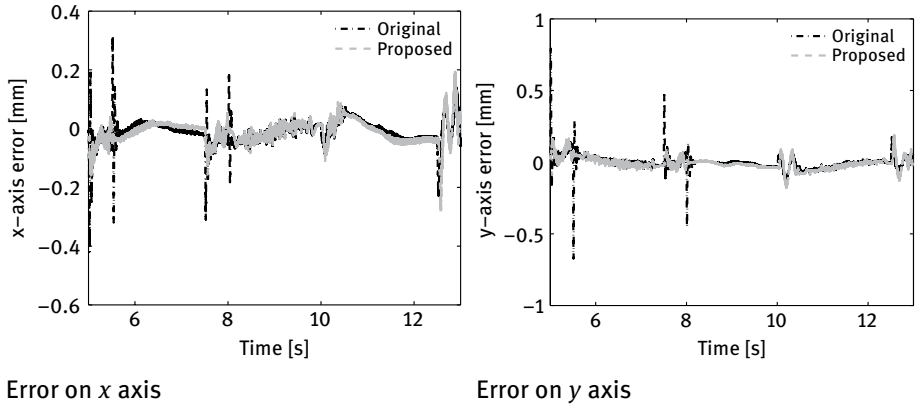Error on x axis   Error on y axis

Fig. 9. Reference Cartesian trajectory used in experiments.

The feedback gains of the controller have been experimentally tuned using the trial-and-error technique. Usually, manipulators are not equipped with velocity sensors, therefore, velocities have to be numerically estimated from positions measurements. In our case, a carefully designed lead-lag filter is used to estimate the velocities.

Figure 9 displays the Cartesian tracking performance of the traveling plate on both x and y axes. It can be clearly seen that in the case of original trajectories, the discontinuities involve a poor tracking performance. This is more noticeable at the beginning and the end of the circle and the ellipse closed shapes which may lead to high frequency vibrations. However, if we check the obtained performance with the proposed approach, we can clearly observe the improvements in terms of tracking errors at the end and starting points. The proposed trajectories are accurately tracked thanks to the removed discontinuities. The improvements are more observable on the starting and end points of the circle and ellipse trajectories ($t = 5, 5.5, 7.5$ and $8s$). These results were expected since the main purpose of this paper was to propose a technique to remove these discontinuities from the trajectories generated by means of classical analytical functions. These discontinuities are a major source of tracking errors.

The generated control inputs when using the proposed method as well as those generated by the classical one are shown in Figs. 11 and 10 respectively. As expected, the controller generates very high torques when the reference trajectories contain discontinuities, because the drives need to generate high torques in order step from zero to a certain velocity in a very short time, which is in practice very delicate.
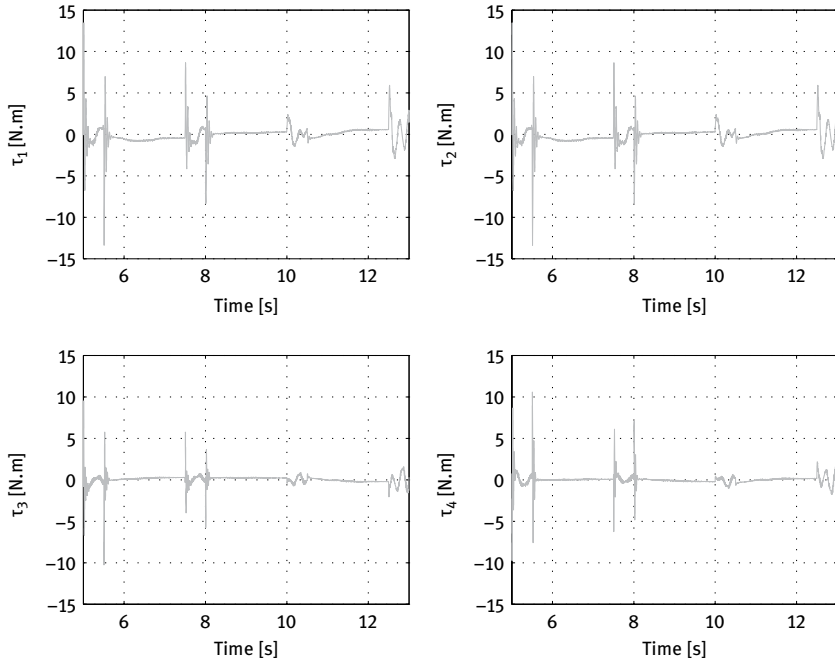
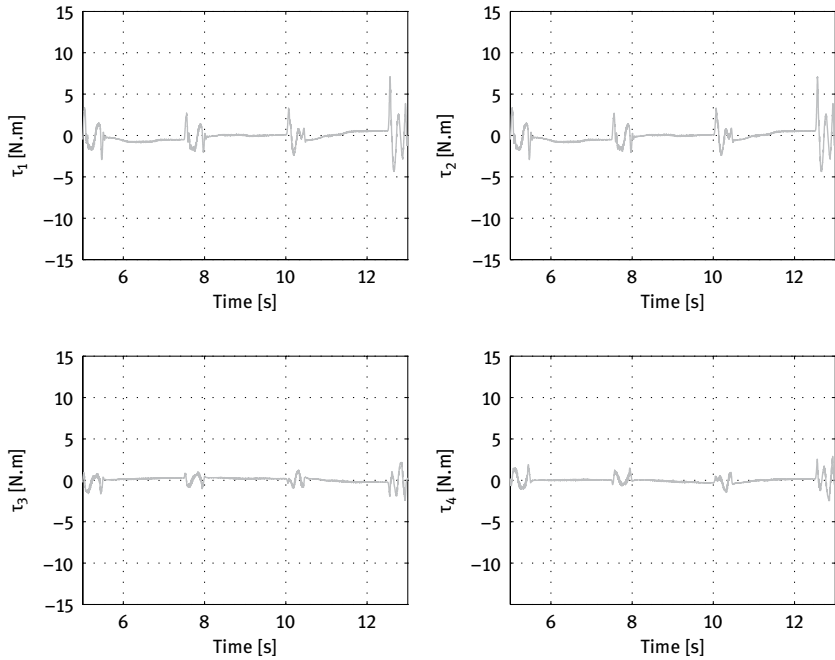**Fig. 10.** Control inputs when using discontinuous trajectories.

Fig. 11. Control inputs when using the proposed C^2 trajectories.

6 Conclusions and Future Work

Throughout this paper, we investigated the generation of continuous geometric closed-shape reference trajectories. Moreover, to accurately track these trajectories, a novel model-based controller in joint space has been proposed. The proposed controller enables the reduction of antagonistic internal forces caused by the unavoidable use of decentralized strategies in the control scheme. The geometric trajectories in question are defined using analytical functions that show inherent discontinuities regarding velocities and accelerations which may be a source of poor tracking. For this reason, we proposed in this work an approach to overcome this issue by modifying the motion profile without changing the overall geometric shape of the trajectory in operational space. Furthermore, to overcome the phenomenon of internal forces, a novel extended PD controller with computed feedforward was proposed. The computed control inputs were regularized using a projection matrix based on the manipulator's Jacobian matrix to reduce the antagonistic control inputs. This projection enables to significantly reduce the antagonistic internal forces that may damage the mechanical structure. This strategy allows to significantly reduce the energy consumption and to cancel the mechanical vibrations of the mechanical structure. To validate the proposed approaches, real-time experiments have been conducted on a 3-dof planar RA-PKM developed in our laboratory. The proposed trajectory generator demonstrated its superiority over the original one that utilizes discontinuous analytical equations.

Bibliography

[1] Jean-Pierre Merlet. *Parallel Robots*. Kluwer Academic Publishers, Netherlands, 2000.

[2] D. Corbel, M. Gouttefarde, and O. Company. Towards 100G with PKM. Is actuation redundancy a good solution for pick-and-place?. In *Proceedings of The IEEE Int. Conf. on Robotics and Automation (ICRA'10)*, 4675–4682, Anchorage-Alaska, May 2010.

[3] Ilian Bonev. Delta Parallel Robot – the Story of Success. *ParalleMIC*, May 2001.

[4] Marconi. The Gadfly manipulator. *Research Report 732*, Marconi Research Center, 1985.

[5] S. Macfarlane and E. A. Croft. Jerk-bounded manipulator trajectory planning: design for real-time applications. *IEEE Transactions on Robotics and Automation* 19(1):42–52, 2003.

[6] Y. Liu, C. Wang, J. Li and L. Sun. Time-Optimal Trajectory Generation of a Fast-Motion Planar Parallel Manipulator. In *Proceedings of The IEEE Int. Conf. on Intelligent Robots and Systems (IROS'06)*, 754–759, Beijing-China, October 2006.

[7]   C. Barnard, S. Briot and S. Caro. Trajectory generation for high speed pick and place robots. In *Proceedings of The ASME 2012 11th Biennial Conference On Engineering Systems Design And Analysis*, Nantes-France, July 2012

[8]   L. E. Bruzzone, R.M Molfino and R. P. Razzoli. Modeling and design of a parallel robot for laser-cutting applications. In *Proceedings of the IASTED International Conference on Modelling, Identification, and Control (MIC 2002)*, 518–522, Innsbruck-Austria, February 2002.

[9]   H. Chanal. *Etude de l'emploi des machines outils à structure parallèle en usinage*, PhD thesis, Université Blaise Pascal, Clermont-Ferrand-France, 2006.

[10] Y. LI and Q. XU. Design and development of a medical parallel robot for cardiopulmonary resuscitation. *IEEE/ASME Transactions on Mechatronics*, 12(3):265–273, 2007.

[11] H. J. Su, P. Dietmaier and J. M. McCarthy. Trajectory planning for constrained parallel manipulators. *Journal of mechanical design*, 125(4):709–716, 2003.

[12] F. Paccot, N. Andreff and P. Martinet. A Review on the Dynamic Control of Parallel Kinematic Machines: Theory and Experiments. *The International Journal of Robotics Research*, 28(3):395–416, 2009.

[13] J. F. He, H. Z. Jiang, D. C. Cong, Z. M. Ye and J. W. Han. A Survey on Control of Parallel Manipulator. *Key Engineering Materials*, 339:307–313, 2007.

[14] H. Cheng, Y. K. Yiu and Z. Li. Dynamics and Control of Redundantly Actuated Parallel Manipulators. *IEEE/ASME Transactions on Mechatronics*, 8(4):483–491, 2003.

[15] A. Müller and T. Hufnagel. A projection method for the elimination of contradicting control forces in redundantly actuated PKM. In *Proceedings of The IEEE Int. Conf. on Robotics and Automation (ICRA'11)*, 3218–3223, Shanghai-China, May 2011.

[16] F. Reyes and R. Kelly. Experimental evaluation of model-based controllers on a direct-drive robot arm. *Mechatronics*, 11(3):267–282, 2001.

[17] V. Van Der Wijk, S. Krut, F. Pierrot and J. L. Herder. Design and experimental evaluation of a dynamically balanced redundant planar 4-RRR parallel manipulator. *The International Journal of Robotics Research*, 32(6):744–759, 2013.

[18] J. Wu, J. Wang and Z. You. A comparison study on the dynamics of planar 3-DOF 4-RRR, 3-RRR and 2-RRR parallel manipulators. *Robotics and Computer Integrated Manufacturing*, 27(1):150–156, 2011.

[19] V. Van Der Wijk, S. Krut, F. Pierrot and J. L. Herder. Generic Method for Deriving the General Shaking Force Balance Conditions of Parallel Manipulators with Application to a Redundant Planar 4-RRR Parallel Manipulator. In *Proceedings of The 13th World Congress in Mechanism and Machine Science*, Guanajuato-Mexico, 2011.

Biographies

Moussab Bennehar received his B.Sc. and M.Sc. degrees in electronics from the university of Constantine, Algeria, in 2012. He is currently a Robotics PhD student at Laboratoire d'Informatique, de Robotique et de Microélectronique de Montpellier (LIRMM - UMR 5506) in the Montpellier Laboratory of Computer Science, Robotics, and Microelectronics, France. His research is focused on trajectory generation and control of multibody systems. His PhD thesis is focused on advanced control techniques of parallel kinematic manipulators.

Ahmed Chemori received his M.Sc. and Ph.D. degrees, respectively in 2001 and 2005, both in automatic control from the Grenoble Institute of Technology. He has been a post-doctoral fellow with the automatic control laboratory of Grenoble in 2006. He is currently a tenured research scientist in Automation and Robotics at the Montpellier Laboratory of Computer Science, Robotics, and Microelectronics. His research interests include nonlinear, adaptive and predictive control and their applications in humanoid robotics, underactuated systems, parallel robots and underwater vehicles.

Sébastien Krut received the M.S. degree in mechanical engineering from the Pierre and Marie Curie University, Paris, France, in 2000 and the Ph.D. degree in automatic control from the Montpellier University of Sciences, Montpellier, France, in 2003. He has been a Post-doctoral fellow with the Joint Japanese-French Robotics Laboratory (JRL) in Tsukuba, Japan in 2004. He is currently a tenured research scientist in Robotics for the French National Centre for Scientific Research (CNRS), at the Montpellier Institute of Informatics, Microelectronics and Robotics (LIRMM in French), Montpellier, France. His research interests include design and control of robotic systems in general, and more specifically of parallel manipulators.

François Pierrot is a senior researcher in robotics for CNRS. His research interests include the creation of innovative robots and he considers both mechanical design and control strategies.